HHS Public Access

Author manuscript

J Neurovirol. Author manuscript; available in PMC 2020 June 01.

Published in final edited form as:

J Neurovirol. 2019 June ; 25(3): 313–323. doi:10.1007/s13365-018-0714-5.

White Matter Microstructure among Perinatally HIV-infected Youth: A Diffusion Tensor Imaging Study

Manoj K. Sarma[1], **Margaret A. Keller**[2,3], **Paul M. Macey**[4,5], **David E. Michalik**[6], **Judy Hayes**[3], **Karin Nielsen-Saines**[7], **Jaime Deville**[7], **Joseph A. Church**[8], **Irwin Walot**[9], and **M. Albert Thomas**[1]

[1]Radiological Sciences, David Geffen School of Medicine at UCLA, Los Angeles, CA, United States [2]Pediatrics, Los Angeles County Harbor-UCLA Medical Center, Torrance, CA, United States and [3]Los Angeles Biomedical Research Institute at Harbor-UCLA Medical Center, Torrance, CA, United States [4]Brain Research Institute, UCLA School of Medicine, Los Angeles, CA, United States [5]UCLA School of Nursing, Los Angeles, CA, United States [6]Infectious Diseases-Pediatrics, Miller Children's Hospital of Long Beach, Long Beach, CA, United States [7]Pediatrics, David Geffen School of Medicine at UCLA, Los Angeles, CA, United States [8]Pediatrics, Keck School of Medicine at University of Southern California, Children's Hospital Los Angeles, Los Angeles, CA, United States [9]Radiology, Los Angeles County Harbor-UCLA Medical Center, Torrance, CA, United States

Abstract

We evaluated white matter microstructure integrity in perinatally HIV-infected youths receiving cART compared to age- and gender- matched healthy youths through DTI metrics using voxel-based morphometry (VBM). We investigated fourteen perinatally HIV infected patients (age 17.92± 2.5 years) on cART and seventeen healthy youths (HC) (age 17.95± 3.0 years) using a 3T MRI scanner. Four DTI derived metrics were fractional anisotropy (FA), mean diffusivity (MD), axial diffusivity (AD) and radial diffusivity (RD). Statistical analysis was done with voxel-based analysis of covariance (ANCOVA), with age and gender as covariates. Region-of-interest secondary analyses for the statistical significant regions were also performed. Regional increases in FA in the PHIV youth were found in left middle frontal gyrus, right precuneus, right lingual gyrus and left supramarginal gyrus. Increased MD was found in the right precentral gyrus while decreased MD was found in the white matter of the right superior parietal lobule and right inferior temporal gyrus/fusiform gyrus. Regions of increased/decreased RD overlapped with regions of increased/decreased MD. Both increased and decreased AD were found in three to four regions respectively. The regional FA, MD, RD and AD values were consistent with the voxel-based analysis findings. The findings are mostly consistent with previous literature, but increased FA has not been previously reported for perinatally HIV-infected youths. Potentially early and prolonged therapy in our population may have contributed to this new finding. Both toxicity of antiretroviral

Address for Correspondence: M. Albert Thomas, Ph.D., Radiological Sciences, David Geffen School of Medicine at UCLA, 10833 Le Conte Avenue, Los Angeles, CA 90095-1721, Tel: (310) 206 4191, Fax: (310) 825 5837, athomas@mednet.ucla.edu.

Conflict of interest: No conflict of interest declared.

therapy and indolent infection must be considered as causative factors in the DTI metric changes that we have observed.

Keywords

Brain; human immunodeficiency virus (HIV); combination anti-retroviral therapy (cART); diffusion tensor imaging (DTI); fractional anisotropy (FA); mean diffusivity (MD); radial diffusivity (RD); axial diffusivity (AD); voxel based morphometry (VBM)

Introduction:

Progress in the treatment of human immunodeficiency virus (HIV) infection with combination antiretroviral therapy (cART) has transformed HIV into a chronic disease (Lee et al. 2006; Moore and Chaisson 1999; Palella et al. 1998; Patel et al. 2008) in both adults and perinatally HIV-infected (PHIV) children and youths. Despite the success of cART, current studies show many HIV-infected individuals who continue to have neurocognitive difficulties and may experience indolent ongoing brain injury despite cART medications (Winston et al. 2015; Liner et al. 2010; Whitehead et al. 2014; Kolson 2017; Laughton et al. 2013).

As discussed in recent reviews (Ellis et al. 2009; Connolly et al. 2005; Wood et al. 2009; Robertson et al. 2012; Musielak and Fine 2016; Ellis et al. 2007), HIV damage to the central nervous system (CNS) may be the result of direct infection with HIV, opportunistic infections, or toxicity from antiretroviral medications. Persistent inflammation may also be a cause of neurological sequelae. Neuroimaging could potentially be an effective, noninvasive tool for monitoring the status of the CNS in chronic HIV infection. Potentially, imaging biomarkers could indicate the need for a change in therapy before neurocognitive findings are detectable using neurocognitive assessments. To date, neuroimaging studies, based on structural brain MRI, show neurological abnormalities in perinatally HIV-infected children including ventricular enlargement, and atrophy of cortical and subcortical regions (Hoare et al. 2014; Johann-Liang et al. 1998; Ackermann et al. 2014). In our previous brain structural study using voxel based morphometry (Sarma et al. 2013), we found white matter (WM) atrophy in perinatally HIV-infected youths in brain areas including the bilateral posterior corpus callosum (CC), bilateral external capsule, bilateral ventral temporal WM, mid cerebral peduncles, and basal pons.

Diffusion tensor imaging (DTI), an MRI technique that provides indices of diffusion of water between tissues (Basser and Pierpaoli 1996), also can be used to study cerebral white matter (WM) microstructure and subcortical inflammatory changes associated with HIV infection (Thomason and Thompson 2011; Pomara et al. 2001; Stebbins et al. 2007; Hoare et al. 2012). Diffusion data allow characterization of water diffusivity with the diffusion tensor at each voxel, and a variety of quantitative indices can be calculated from the DTI tensor that reflect the magnitude and orientation of water diffusion, which are influenced by the underlying structure. Two commonly used DTI metrics for characterizing WM integrity are fractional anisotropy (FA) and mean diffusivity (MD). FA is a normalized measure (values between 0 and 1) indicating directional selectivity of water diffusion, and represents

the degree of alignment of the underlying fibers in a voxel (Beaulieu 2002). FA is higher in organized WM tracts, reflecting slow diffusivity perpendicular to the fibers and a fast diffusivity along them (Pierpaoli et al. 1996). FA is lower in less ordered tissues, such as gray matter (GM), while it approaches zero in cerebrospinal fluid (CSF) (Wozniak and Lim 2006). MD can serve as a measure of generalized tissue breakdown, and represents the average magnitude of diffusive motion in all directions. MD is affected by cell size, shape, and integrity (Pierpaoli et al. 1996) and declines with increasing tissue barriers, such as cell membranes and myelin sheaths (Basser and Pierpaoli 1996). Axial diffusivity (AD) and radial diffusivity (RD) are additional DTI derived metrics respectively measuring water diffusivity parallel and perpendicular to the principal direction of the WM fibers providing greater detail on microstructural properties. Increased RD is associated with demyelination (Song et al. 2005) and dysmyelination (Song et al. 2002), whereas decreased AD occurs with axonal damage (Loy et al. 2007).

These DTI measures in clinical populations serve as markers of pathology and change over time, and in vertically HIV-infected children and youths could provide information on the location of white matter microstructural changes that correlate with clinical variables. However, it is unclear how accurately the directional diffusivities relate to specific pathologies in perinatally HIV-infected children and youths, especially with regard to discerning the effects of chronic lifelong infection and prolonged treatment. Although DTI has been used in HIV- infected adults to document abnormal WM microstructure (Pomara et al. 2001; Stebbins et al. 2007; Berger and Avison 2001; Stubbe-Drger et al. 2012; Wright et al. 2012; Hoare et al. 2011), there are relatively few groups who have studied DTI in perinatally HIV-infected youth (Hoare et al. 2012; Hoare et al. 2014; Hoare et al. 2015; Cohen et al. 2016; Jahanshad et al. 2015).

In the present study, using DTI metrics (MD, FA, AD and RD), we evaluated the WM microstructure integrity in perinatally HIV-infected youths receiving cART compared to age- and gender-matched healthy controls utilizing voxel-based analysis, which are closely related to voxel-based morphometry (VBM) (Ashburner and Friston 2000). VBM-type analyses provides a global and comprehensive assessment of group differences with voxel-by-voxel statistical comparisons throughout the brain. Being an automated technique, it has been noted to be reliable and reproducible. Detection of WM damage could be an indicator of future neurodevelopmental deficits and may guide clinical treatment whereas absence of measurable differences could be reassuring. Furthermore, we sought to examine any association between white matter microstructure and HIV disease and treatment variables among these youths, including higher current viral load, highest known viral load, lowest known CD4 count, lowest known CD4 %, current CD4 count, age at initiation of treatment for HIV, and length of HIV treatment.

Materials and Methods:

Subjects

We investigated fourteen perinatally HIV infected patients (age 17.92± 2.5 years, range 14.3–22.5) and seventeen healthy controls (HC) (age 17.95 years± 3.0, range 13.4–23.6). The perinatally HIV-infected subjects were recruited from four medical centers providing

care for these youths in the Los Angeles area: Los Angeles County Harbor-UCLA Medical Center (Torrance, CA), Miller Children's Hospital of Long Beach (Long Beach, CA), David Geffen School of Medicine at UCLA (Los Angeles, CA), and Children's Hospital Los Angeles (Los Angeles, CA). The healthy controls were recruited from family members of the subjects, the general pediatric clinic at Los Angeles County Harbor-UCLA Medical Center, the UCLA university community, local junior college community, the Los Angeles Biomedical Research Institute community and the general community. The protocol was approved by the institutional review board (IRB) both at Los Angeles Biomedical Research Institute at Harbor-UCLA Medical Center and at the University of California at Los Angeles. All subjects completed study procedures voluntarily. Signed informed consent was obtained from subjects 18 years or older and from the parents or legal guardians of younger subjects. Subjects between the ages of 13–17 years signed an assent for participation.

Study criteria—Study inclusion criteria were similar to our previous studies (Nagarajan et al. 2012; Sarma et al. 2013) and consisted of the following: (1) 13–30 years of age; (2) perinatal acquisition of HIV or confirmation of HIV-uninfected status with Ora–Quick (OraSure Technologies, Bethlehem, PA 18015) buccal scraping (for HIV− subjects); (3) current treatment with combination antiretroviral medication for HIV-infected subjects; (4) post-menarchal status for all females since all females were studied in the follicular phase of the menstrual cycle to reduce variability; (5) right-hand dominance; and (6) negative urine pregnancy test if female. We excluded participants if they had: (1) a history of CNS opportunistic infection or other CNS condition (other than HIV); (2) severe metabolic disturbances, such as hepatic or renal failure; (3) metallic implants or braces or permanent retainers or other MRI exclusions; (4) claustrophobia; (5) Attention Deficit/Hyperactivity Disorder; (6) pregnancy (by interview and urine pregnancy test before scanning); (7) smoking (nicotine); (8) alcohol or other substance use/abuse including marijuana; (9) active psychiatric diagnosis; (10) severe school difficulties in control subjects; (11) chronic medication other than asthma medication in control subjects; (12) female subjects in luteal phase of menstrual cycle; and (13) hepatitis C infection.

Each subject fulfilling the study criteria was assessed with DTI scans. For HIV+ subjects, the following additional data were collected from the chart review: age at first treatment for HIV; HIV viral load close to time of testing; highest known viral load; CD4 T cell counts close to time of testing; lowest known CD4; lowest known CD4%; current antiretroviral therapy; known presence of HIV encephalopathy; and history of maternal substance abuse during pregnancy.

MRI

All MRI studies were performed using a 3T MRI scanner (Siemens Medical Solution, Erlangen, Germany), using a 16-channel phased-array head 'receive' coil. To minimize head movement, foam pads were placed on either side of the head. DTI was performed using a single-shot multi-section spin-echo echo-planar pulse sequence [repetition time (TR) = 10,000 ms; echo-time (TE) = 90 ms; flip angle = 90°; average = 4, gradient duration = 20 ms in the axial plane, with a 130 × 130 matrix size, 256 × 256 mm^2 field of view (FOV), 2.0 mm slice thickness, 75 slices, 0 interslice gap, and a readout bandwidth of 1347 Hz/pixel.

For each slice, diffusion gradients were applied along 64 independent orientations with b = 700 sec/mm^2 after the acquisition of b = 0 sec/mm^2 (b0) images. High-resolution 3-dimensional T1-weighted anatomical scans were collected using a magnetization-prepared rapid-acquisition-gradient-echo pulse sequence (TR = 2200 ms; TE = 2.2 ms; inversion time = 900 ms; flip angle = 9°; matrix size = 256 × 256; FOV = 240 × 240 mm; slice thickness = 1.0 mm; number of slices = 176).

Data Processing

The statistical parametric mapping package SPM12 (https://www.fil.ion.ucl.ac.uk/spm/software/spm12/), DTI-Studio (Jiang et al. 2006), MRIcroN (Rorden et al. 2007), and custom MATLAB-based software were used for evaluation of images, data processing, and analyses. The Diffusion Toolbox for SPM was used to process the DTI data. The diffusion tensor was calculated at each voxel, from which whole-brain maps of FA, MD, AD and RD were derived. The normalization parameters derived from b0 images were used to normalize DTI maps, which were then smoothed with an 8 mm Gaussian filter.

Region-of-interest (ROI) analyses were used to determine average values for the diffusivity parameters from those brain locations that show significant **differences** between PHIV-infected youths and control groups, based on VBM analysis. Regional ROI masks were created for distinct brain regions using clusters identified by VBM procedures, and used to calculate average FA, MD, RD, and AD values using normalized and smoothed maps.

Statistical Analyses

To define regional differences in FA, MD, AD and RD values between patients and controls, statistical analysis was done with VBM (Ashburner and Friston 2000) using analysis of covariance (ANCOVA) model with age and gender as covariates. We established significance at a height threshold of $p < 0.001$ (uncorrected) and an extent threshold of 30 voxels.

Statistical Package for the Social Sciences (SPSS, V 24.0, IBM, Chicago, IL) software was used to examine demographic and regional diffusivity parameters from ROI analyses. The independent samples *t*-tests were performed to examine age, and gender differences between PHIV-infected and healthy control groups. The average values for FA, MD, RD, and AD from ROI analyses for different locations were compared between PHIV-infected youths and healthy controls with multivariate ANCOVA (covariate: age and gender).

Results:

Demographic and clinical data of PHIV and control subjects are summarized in Table 1. No significant differences were found in age and gender between the two groups. Ten of the fourteen subjects had a log viral load < 1.68 while receiving cART. Of the 14 patients, five had evidence of HIV encephalopathy. For 12 subjects, there was no evidence of maternal substance abuse during pregnancy. For the remaining two patients, one had evidence of maternal substance abuse and the information was unknown for the other.

Voxel-wise comparisons of DTI matrices FA, MD, RD and AD revealed significant regional group differences. Regional increases in FA in the PHIV youth group compared to the HC group were found in 4 regions (Figure 1), including left middle frontal gyrus, right precuneus, right lingual gyrus and left supramarginal gyrus. No regions showed decreased FA values in PHIV youths compared to HC. Voxel-wise comparisons of MD between the groups revealed regions of significantly decreased and increased diffusivity in the PHIV subjects compared to the HC subjects (Figure 2). Increased mean diffusivity was found in the right precentral gyrus in the PHIV subjects. Decreased mean diffusivity was found in PHIV subjects in 2 regions, including the white matter of the right superior parietal lobule and right inferior temporal gyrus/fusiform gyrus. Although both increased and decreased MD was observed in selected cerebral locations in the PHIV youths, there was no direct overlap of specific lobar locations.

Regions of increased/decreased RD in the PHIV group overlapped with regions of increased/decreased MD in the same group (Figure 3). Specifically, right precentral gyrus showed increased, and right superior parietal lobule and inferior temporal gyrus/fusiform gyrus showed decreased RD in the PHIV subjects compared to HC. Figure 4 shows regions of increased/decreased AD in PHIV youths relative to healthy control subjects. Three brain sites in PHIV patients showed significantly increased AD values, including left putamen, left parietal operculum, and cerebellar vermal lobules. Decreased AD was observed in the right inferior temporal gyrus/fusiform gyrus, right posterior cingulate gyrus, right superior parietal lobule, and left precuneus. Two regions of decreased AD in the PHIV group overlapped with regions of decreased MD and RD. These regions included right inferior temporal gyrus/fusiform gyrus, and right superior parietal lobule. The regional FA, MD, RD and AD values derived from multiple brain areas from PHIV-infected youths and healthy controls are presented in Table 2. The **ROI analysis** results are consistent with **the** voxel-based analysis findings **reported above**.

Association of disease markers with DTI parameters among PHIV youth

Scan CD4 count, lowest known CD4, lowest known CD4%, scan viral load, highest known viral load, length of first treatment, age at diagnosis, and age at first treatment were not associated with either of FA, MD, RD and AD when age and gender were used as covariates of interest.

Discussion:

In this study, we used VBM-based DTI analysis to study the integrity of WM, and the relationship between DTI measures and clinical parameters in perinatally HIV-infected youths receiving current cART. Results presented here indicate that PHIV-infected youths have DTI-derived microstructural alterations compared to healthy controls in several brain regions. In PHIV-infected youths, we found both decreased and increased MD. Differences in FA were more consistent, with increases noted in the PHIV youths compared to the healthy controls. Regions displaying significantly increased and decreased MD in the PHIV-infected youths were also found to have significantly increased and decreased RD and AD compared to the healthy controls. Although both increased and decreased MD, RD and AD

values were observed in several cerebral locations in the PHIV-infected youths, no direct overlap of specific locations with increased values with that of decreased were noticed.

Both lower and higher FA have been reported previously in HIV-infected adults (Pomara et al. 2001; Hoare et al. 2011; Wu et al. 2006; Thurnher et al. 2005; Li et al. 2010), but this is the first report showing increased FA in perinatally HIV–infected youths although another study with a similar population to our own found decreased FA using different techniques (total brain FA and tractography) (Uban et al. 2015). Hoare et al. (Hoare et al. 2015) compared DTI metrics with clinical parameters in a younger population than ours receiving cART. In that study, decreased FA was associated with being on a second line regimen and younger age. Inclusion criteria was cART for a minimum of 6 months. In contrast, our population had been treated for an average of 155 months. Another group (Ackermann et al. 2016) also found lower FA in younger (age 5 years) HIV-infected children with predominant involvement of the corticospinal tracts while Jankiewicz et al. (Jankiewicz et al. 2017) studied 7 year old children with HIV and found two regions with lower FA.

Our finding of **higher** FA may represent increased white-matter integrity and/or myelination **or microscopic deficits of axonal structures or decreases in axonal diameter, packing density, and branching** in those areas. When myelinated nerve sheaths are affected in a patient population, they may exhibit excessive hyperplasia leading to a high FA value of WM. This may contribute to cognitive deficits often seen in PHIV youths (Wood et al. 2009; Hoare et al. 2012; Nagarajan et al. 2012; Cohen et al. 2015). A **similar interpretation was made for increased FA found in Williams Syndrome (**Hoeft et al. 2007**) and obsessive-compulsive disorder (**Lochner et al. 2012**), with the changes potentially associated with anomalous cognitive function in the two conditions.** Similar to our findings, Stebbins et al. (Stebbins et al. 2007) also found increases in FA in adult HIV patients and suggested an alternate hypothesis. According to these investigators, loss of the complexity of the white-matter matrix in those regions may lead to increased FA. FA can be high in a voxel which contains only parallel white matter fibers. A damaged matrix may result in loss of crossing and leave the parallel fibers intact resulting in a paradoxical increase in FA. One indicator of such a process would be an increase in MD, a measure of tissue damage, in the same WM regions (Hoare et al. 2011; Thurnher et al. 2005). We did not observe significantly increased MD together with the increased FA in the same regions to support this hypothesis.

Another possible explanation for higher FA is increases in fiber tract density. FA is associated with fiber tract density in the owl monkey brain (Choe et al. 2012). This possibility could be investigated further in our data set using fiber tracking algorithms such as FACT (Mori et al. 1999).

Our findings of variable MD changes in PHIV youths relative to healthy controls may account for previous discordant reports of changes in DTI parameters in this population (Pomara et al. 2001; Uban et al. 2015; Stebbins et al. 2007; Pfefferbaum et al. 2007; Chang et al. 2008; Chen et al. 2009). Stebbins et al. (Stebbins et al. 2007) found widespread increases noted in the HIV-seropositive sample compared to the HIV-seronegative sample. Pomara et al. (Pomara et al. 2001) observed no significant differences in MD, but found trend of both increased and decreased MD in HIV+ patients compared to healthy controls.

Most of these studies were on older patients. Increased MD may represent neurodegeneration of white matter, where neuronal loss during neurodegeneration corresponds to increased water molecules, likely resulting in higher MD (Uban et al. 2015; Cho et al. 2008) and can be a sensitive indicator of developmental problems observed in some of the PHIV-infected youth (Filippi et al. 2003). Smaller WM volumes have been observed among PHIV-infected youths in our previous study (Sarma et al. 2013) which support this hypothesis. Another reason for increased MD may be inflammation. Ongoing detectable neuro inflammation (Anthony et al. 2005) has been reported in HIV patients even after the introduction of highly active cART. Inflammatory activity may be a marker of neurological progression from asymptomatic to symptomatic disease stages in HIV (Chang et al. 2004). Ragin et al. (Ragin et al. 2006) reported that elevation of macrophage chemoattractant protein-1 (MCP-1), an inflammatory chemokine, has been correlated with increased MD in the centrum semiovale, the putamen, and caudate of patients with HIV infection.

Higher RD in PHIV-infected youths may reflect failure of the cells to develop fully and create the sheath around the axon resulting in less myelination of tracts (Chen et al. 2009). AD is thought to reflect water diffusivity parallel to axonal fibers and increased axial diffusivity is usually associated with a better WM integrity. However, co-occurring with higher RD as we have found, it may represent simultaneous axonal and myelin degeneration (Roosendaal et al. 2009; Metwalli et al. 2010).

Observed reduction in diffusivity measures (MD, AD, and RD) in PHIV-infected youths in our study are in agreement with the finding by Wright et al. (Wright et al. 2012) on elder HIV+ patients receiving cART. According to these investigators, decreased diffusivity measures may reflect macrophage and microglia infiltration due to active viral replication within the CNS or alternatively, there may be increased cytotoxic edema. As a result, the free path of water diffusion may be decreased by the presence of inflammatory cells and surrounding debris (Wright et al. 2012; Wang et al. 2011).

Though no correlation was found in our study between diffusivity changes and duration of therapy, it is to be noted that all PHIV-infected youths in our study were receiving cART at the time of the MRI scan. cART may effectively suppress the HIV systemic burden, but poor penetration of some antiretroviral medications into the CNS may provide insufficient protection. Long-term cART regimens may cause mitochondrial toxicity, impaired neurogenesis and lead to neuronal loss (Marra et al. 2009; Robertson et al. 2010). These findings suggest that a longer HIV treatment may be associated with potential neurotoxicity in the brains of PHIV-infected youths, which may affect the anisotropy and diffusivity parameters.

Limitations:

Limitations of our study include the relatively small sample size, and the cross-sectional nature of the data, which limits our ability to assess the impact of HIV on brain development over time. In addition, cognitive analysis was not a part of our analysis and intrinsically, we are not able to address the question of whether changes in diffusion parameters exhibit an

early marker of consequent decline in cognitive abilities. Our healthy controls were matched for age and sex to PHIV-infected youth, accounting for the possible interactions of age and gender allowing for meaningful group comparisons. Despite these potential limitations of the study, our results may shed light on white matter integrity damage in PHIV-patients during a longer duration of therapy.

Conclusion:

In PHIV-infected youths, we found white matter integrity changes in terms of increased FA and both increased and decreased MD, RD and AD. Greater HIV-related disease severity early in life may impact organization and/or myelination of underlying white matter microstructure in these youths. Larger cohorts and longitudinal studies are needed to improve our understanding of the pathogenesis of cerebral injury in perinatally HIV-infected youths.

Acknowledgement:

This research was supported by research grants from the National Institute of Neurological Disorders and Stroke (NINDS) 1R21NS08064901A1, 1R21NS09095601A1 and 1R21NS06062001A1. We also acknowledge the scientific support of Dr. Rajakumar Nagarajan.

References:

Ackermann C, Andronikou S, Laughton B, Kidd M, Dobbels E, Innes S, van Toorn R, Cotton M (2014) White matter signal abnormalities in children with suspected HIV-related neurologic disease on early combination antiretroviral therapy. Pediatr Infect Dis J 33:e207–212. doi: 10.1097/INF.0000000000000288 [PubMed: 24595047]

Ackermann C, Andronikou S, Saleh MG, Laughton B, Alhamud AA, van der Kouwe A, Kidd M, Cotton MF, Meintjes EM (2016) Early Antiretroviral Therapy in HIV-Infected Children Is Associated with Diffuse White Matter Structural Abnormality and Corpus Callosum Sparing. AJNR Am J Neuroradiol 37:2363–2369. doi: 10.3174/ajnr.A4921 [PubMed: 27538904]

Anthony IC, Ramage SN, Carnie FW, Simmonds P, Bell JE (2005) Influence of HAART on HIV-related CNS disease and neuroinflammation. J Neuropathol Exp Neurol 64:529–536 [PubMed: 15977645]

Ashburner J, Friston KJ (2000) Voxel-based morphometry--the methods. Neuroimage 11:805–821. doi: 10.1006/nimg.2000.0582 [PubMed: 10860804]

Basser PJ, Pierpaoli C (1996) Microstructural and physiological features of tissues elucidated by quantitative-diffusion-tensor MRI. J Magn Reson B 111:209–219. doi: 10.1.1.162.3203 [PubMed: 8661285]

Beaulieu C (2002) The basis of anisotropic water diffusion in the nervous system - a technical review. NMR Biomed 15:435–455. doi: 10.1002/nbm.782 [PubMed: 12489094]

Berger JR, Avison MJ (2001) Diffusion tensor imaging in HIV infection: what is it telling us?. AJNR Am J Neuroradiol 22:237–238. [PubMed: 11156760]

Chang L, Lee PL, Yiannoutsos CT, Ernst T, Marra CM, Richards T, Kolson D, Schifitto G, Jarvik JG, Miller EN, Lenkinski R, Gonzalez G, Navia BA; HIV MRS Consortium (2004) A multicenter in vivo proton-MRS study of HIV-associated dementia and its relationship to age. Neuroimage 23:1336–1347. DOI: 10.1016/j.neuroimage.2004.07.067 [PubMed: 15589098]

Chang L, Wong V, Nakama H, Watters M, Ramones D, Miller EN, Cloak C, Ernst T (2008) Greater than age-related changes in brain diffusion of HIV patients after 1 year. J Neuroimmune Pharmacol 3:265–274. doi: 10.1007/s11481-008-9120-8 [PubMed: 18709469]

Chen Y, An H, Zhu H, Stone T, Smith JK, Hall C, Bullitt E, Shen D, Lin W (2009) White matter abnormalities revealed by diffusion tensor imaging in non-demented and demented HIV+ patients. Neuroimage 47:1154–1162. doi: 10.1016/j.neuroimage.2009.04.030 [PubMed: 19376246]

Cho H, Yang DW, Shon YM, Kim BS, Kim YI, Choi YB, Lee KS, Shim YS, Yoon B, Kim W, Ahn KJ (2008) Abnormal integrity of corticocortical tracts in mild cognitive impairment: a diffusion tensor imaging study. J Korean Med Sci 23:477–483. doi: 10.3346/jkms.2008.23.3.477 [PubMed: 18583886]

Choe AS, Stepniewska I, Colvin DC, Ding Z, Anderson AW (2012) Validation of diffusion tensor MRI in the central nervous system using light microscopy: Quantitative comparison of fiber properties. NMR Biomed 25:900–908. doi: 10.1002/nbm.1810 [PubMed: 22246940]

Cohen S, Caan MW, Mutsaerts HJ, Scherpbier HJ, Kuijpers TW, Reiss P, Majoie CB, Pajkrt D (2016) Cerebral injury in perinatally HIV-infected children compared to matched healthy controls. Neurology 86:19–27. doi: 10.1212/WNL.0000000000002209 [PubMed: 26561287]

Cohen S, Ter Stege JA, Geurtsen GJ, Scherpbier HJ, Kuijpers TW, Reiss P,Schmand B, Pajkrt D (2015) Poorer cognitive performance in perinatally HIV-infected children versus healthy socioeconomically matched controls. Clin Infect Dis 60:1111–1119. doi: 10.1093/cid/ciu1144 [PubMed: 25516183]

Connolly NC, Riddler SA, Rinaldo CR (2005) Proinflammatory cytokines in HIV disease-a review and rationale for new therapeutic approaches. AIDS Rev 7:168–180. doi: 10.1371/journal.pone.0170063 [PubMed: 16302465]

Ellis R, Langford D, Masliah E (2007) HIV and antiretroviral therapy in the brain: neuronal injury and repair. Nat Rev Neurosci 8:33–44. doi: 10.1038/nrn2040 [PubMed: 17180161]

Ellis RJ, Calero P, Stockin MD (2009) HIV infection and the central nervous system: a primer. Neuropsychol Rev 19:144–151. doi: 10.1007/s11065-009-9094-1 [PubMed: 19415500]

Filippi CG, Lin DD, Tsiouris AJ, Watts R, Packard AM, Heier LA, Uluğ AM (2003) Diffusion-tensor MR imaging in children with developmental delay: preliminary findings. Radiology 229:44–50. DOI: 10.1148/radiol.2291020049 [PubMed: 12920176]

Hoare J, Fouche JP, Phillips N, Joska JA, Donald KA, Thomas K, Stein DJ (2015) Clinical associations of white matter damage in cART-treated HIV-positive children in South Africa. J Neurovirol 21:120–128. doi: 10.1007/s13365-014-0311-1 [PubMed: 25604496]

Hoare J, Fouche JP, Spottiswoode B, Donald K, Philipps N, Bezuidenhout H, Mulligan C, Webster V, Oduro C, Schrieff L, Paul R, Zar H, Thomas K, Stein D (2012) A diffusion tensor imaging and neurocognitive study of HIV-positive children who are HAART-naïve “slow progressors”. J Neurovirol 18:205–212. doi: 10.1007/s13365-012-0099-9 [PubMed: 22552809]

Hoare J, Fouche JP, Spottiswoode B, Sorsdahl K, Combrinck M, Stein DJ, Paul RH, Joska JA (2011) White-Matter damage in Clade C HIV-positive subjects: a diffusion tensor imaging study. J Neuropsychiatry Clin Neurosci 23:308–315. doi: 10.1176/appi.neuropsych.23.3.308 [PubMed: 21948892]

Hoare J, Ransford GL, Philipps N, Amos T, Donald KA, Stein DJ (2014) Systematic review of neuroimaging studies in vertically transmitted HIV positive children and adolescents. Metab Brain Dis 29:221–229. doi: 10.1007/s11011-013-9456-5 [PubMed: 24338026]

Hoeft F, Barnea-Goraly N, Haas BW, Golarai G, Ng D, Mills D, Korenberg J, Bellugi U, Galaburda A, Reiss AL (2007) More is not always better: increased fractional anisotropy of superior longitudinal fasciculus associated with poor visuospatial abilities in Williams syndrome. J Neurosci27:11960–11965. doi: 10.1523/JNEUROSCI.3591-07.2007

Jahanshad N, Couture MC, Prasitsuebsai W, Nir TM, Aurpibul L, Thompson PM, Pruksakaew K, Lerdlum S, Visrutaratna P, Catella S, Desai A, Kerr SJ, Puthanakit T, Paul R, Ananworanich J, Valcour VG; SEARCH 012 and PREDICT Study Groups (2015) Brain Imaging and Neurodevelopment in HIV-uninfected Thai Children Born to HIV-infected Mothers. Pediatr Infect Dis J 34:e211–216. doi: 10.1097/INF.0000000000000774 [PubMed: 26090574]

Jankiewicz M, Holmes MJ, Taylor PA, Cotton MF, Laughton B, van der Kouwe AJW, Meintjes EM (2017) White Matter Abnormalities in Children with HIV Infection and Exposure. Front Neuroanat 11:88. doi: 10.3389/fnana.2017.00088 [PubMed: 29033797]

Jiang H, van Zijl PC, Kim J, Pearlson GD, Mori S (2006) DtiStudio: resource program for diffusion tensor computation and fiber bundle tracking. Comput Methods Programs Biomed 81:106–116. doi: 10.1016/j.cmpb.2005.08.004 [PubMed: 16413083]

Johann-Liang R, Lin K, Cervia J, Stavola J, Noel G (1998) Neuroimaging findings in children perinatally infected with the human immunodeficiency virus. Pediatr Infect Dis J 17:753–754. [PubMed: 9726355]

Kolson D (2017) Neurologic Complications in Persons With HIV Infection in the Era of Antiretroviral Therapy. Top Antivir Med 25:97–101. [PubMed: 28820724]

Laughton B, Cornell M, Boivin M, Van Rie A (2013) Neurodevelopment in perinatally HIV-infected children: a concern for adolescence. J Int AIDS Soc 16:18603. doi: 10.7448/IAS.16.1.18603 [PubMed: 23782482]

Lee GM, Gortmaker SL, McIntosh K, Hughes MD, Oleske JM, Pediatric AIDS Clinical Trials Group Protocol 219C Team (2006) Quality of life for children and adolescents: impact of HIV infection and antiretroviral treatment. Pediatrics 117:273–283. doi: 10.1542/peds.2005-0323 [PubMed: 16452344]

Li Q, Sun J, Guo L, Zang Y, Feng Z, Huang X, Yang H, Lv Y, Huang M, Gong Q (2010) Increased fractional anisotropy in white matter of the right frontal region in children with attention-deficit/hyperactivity disorder: a diffusion tensor imaging study. Neuro Endocrinol Lett 31:747–753. [PubMed: 21196923]

Liner KJ 2nd, Ro MJ, Robertson KR (2010) HIV, antiretroviral therapies, and the brain. Current HIV/AIDS Reports 7:85–91. doi: 10.1007/s11904-010-0042-8 [PubMed: 20425562]

Lochner C, Fouché JP, du Plessis S, Spottiswoode B, Seedat S, Fineberg N, Chamberlain SR, Stein DJ (2012) Evidence for fractional anisotropy and mean diffusivity white matter abnormalities in the internal capsule and cingulum in patients with obsessive-compulsive disorder. J Psychiatry Neurosci 37:193–199. doi: 10.1503/jpn.110059 [PubMed: 22297066]

Loy DN, Kim JH, Xie M, Schmidt RE, Trinkaus K, Song SK (2007) Diffusion tensor imaging predicts hyperacute spinal cord injury severity. J Neurotrauma 24:979–990. doi: 10.1089/neu.2006.0253 [PubMed: 17600514]

Marra CM, Zhao Y, Clifford DB, Letendre S, Evans S, Henry K, Ellis RJ, Rodriguez B, Coombs RW, Schifitto G, McArthur JC, Robertson K; AIDS Clinical Trials Group 736 Study Team (2009) Impact of combination antiretroviral therapy on cerebrospinal fluid HIV RNA and neurocognitive performance. AIDS 23:1359–1366. doi: 10.1097/QAD.0b013e32832c4152 [PubMed: 19424052]

Metwalli NS, Benatar M, Nair G, Usher S, Hu X, Carew JD (2010) Utility of axial and radial diffusivity from diffusion tensor MRI as markers of neurodegeneration in amyotrophic lateral sclerosis. Brain Res 1348:156–164. doi: 10.1016/j.brainres.2010.05.067 [PubMed: 20513367]

Mori S, Crain BJ, Chacko VP, van Zijl PC (1999) Three-dimensional tracking of axonal projections in the brain by magnetic resonance imaging. Ann Neurol 45:265–269. doi: N/A [PubMed: 9989633]

Moore RD, Chaisson RE (1999) Natural history of HIV infection in the era of combination antiretroviral therapy. AIDS 13:1933–1942. doi: 10.1097/00002030-199910010-00017 [PubMed: 10513653]

Musielak KA, Fine JG (2016) An Updated Systematic Review of Neuroimaging Studies of Children and Adolescents with Perinatally Acquired HIV. J Pediatr Neuropsychol 2:34–49. doi: 10.1007/s40817-015-0009-1

Nagarajan R, Sarma MK, Thomas MA, Chang L, Natha U, Wright M, Hayes J, Nielsen-Saines K, Michalik DE, Deville J, Church JA, Mason K, Critton-Mastandrea T, Nazarian S, Jing J, Keller MA (2012) Neuropsychological Function and Cerebral Metabolites in HIV-infected Youth. J Neuroimmune Pharmacol 7: 981–990. doi: 10.1007/s11481-012-9407-7 [PubMed: 23065459]

Palella FJ Jr, Delaney KM, Moorman AC, Loveless MO, Fuhrer J, Satten GA, Aschman DJ, Holmberg SD (1998) Declining morbidity and mortality among patients with advanced human immunodeficiency virus infection. HIV Outpatient Study Investigators. N Engl J Med 338:853–860. doi: 10.1056/NEJM199803263381301 [PubMed: 9516219]

Patel K, Hernán MA, Williams PL, Seeger JD, McIntosh K, Van Dyke RB, Seage GR 3rd; Pediatric AIDS Clinical Trials Group 219/219C Study Team (2008) Long-term effectiveness of highly

active antiretroviral therapy on the survival of children and adolescents with HIV infection: a 10-year follow-up study. Clin Infect Dis 46:507–515. doi: 10.1086/526524 [PubMed: 18199042]

Pfefferbaum A, Rosenbloom MJ, Adalsteinsson E, Sullivan EV (2007) Diffusion tensor imaging with quantitative fibre tracking in HIV infection and alcoholism comorbidity: synergistic white matter damage. Brain 130:48–64. doi: 10.1093/brain/awl242 [PubMed: 16959813]

Pierpaoli C, Jezzard P, Basser PJ, Barnett A, Di Chiro G (1996) Diffusion tensor MR imaging of human brain. Radiology 201:637–648. doi: 10.1148/radiology.201.3.8939209 [PubMed: 8939209]

Pomara N, Crandall DT, Choi SJ, Johnson G, Lim KO (2001) White matter abnormalities in HIV-1 infection: a diffusion tensor imaging study. Psychiatry Res 106:15–24. doi: 10.1016/S0925-4927(00)00082-2 [PubMed: 11231096]

Ragin AB, Wu Y, Storey P, Cohen BA, Edelman RR, Epstein LG (2006) Monocyte chemoattractant protein-1 correlates with subcortical brain injury in HIV infection. Neurology 66:1255–1257. doi: 10.1212/01.wnl.0000208433.34723.65 [PubMed: 16636247]

Robertson K, Liner J, Meeker RB (2012) Antiretroviral neurotoxicity. J Neurovirol 18:388–399. doi: 10.1007/s13365-012-0120-3 [PubMed: 22811264]

Robertson KR, Su Z, Margolis DM, Krambrink A, Havlir DV, Evans S, Skiest DJ; A5170 Study Team (2010) Neurocognitive effects of treatment interruption in stable HIV positive patients in an observational cohort. Neurology 74:1260–1266. doi: 10.1212/WNL.0b013e3181d9ed09 [PubMed: 20237308]

Roosendaal SD, Geurts JJ, Vrenken H, Hulst HE, Cover KS, Castelijns JA, Pouwels PJ, Barkhof F (2009) Regional DTI differences in multiple sclerosis patients. Neuroimage 44:1397–1403. doi: 10.1016/j.neuroimage.2008.10.026 [PubMed: 19027076]

Rorden C, Karnath HO, Bonilha L (2007) Improving lesion-symptom mapping. J Cogn Neurosci 19:1081–1088. DOI: 10.1162/jocn.2007.19.7.1081 [PubMed: 17583985]

Sarma MK, Nagarajan R, Keller MA, Kumar R, Nielsen-Saines K, Michalik DE, Deville J, Church JA, Thomas MA (2013) Regional brain gray and white matter changes in perinatally HIV-infected adolescents. Neuroimage Clin 4:29–34. doi: 10.1016/j.nicl.2013.10.012 [PubMed: 24380059]

Song SK, Sun SW, Ramsbottom MJ, Chang C, Russell J, Cross AH (2002) Dysmyelination revealed through MRI as increased radial (but unchanged axial) diffusion of water. Neuroimage 17:1429–1436. doi:10.1006/nimg.2002.1267 [PubMed: 12414282]

Song SK, Yoshino J, Le TQ, Lin SJ, Sun SW, Cross AH, Armstrong RC (2005) Demyelination increases radial diffusivity in corpus callosum of mouse brain. Neuroimage 26:132–140. doi: 10.1016/j.neuroimage.2005.01.028 [PubMed: 15862213]

Stebbins GT, Smith CA, Bartt RE, Kessler HA, Adeyemi OM, Martin E, Cox JL, Bammer R, Moseley ME (2007) HIV-associated alterations in normal-appearing white matter: a voxel-wise diffusion tensor imaging study. J Acquir Immune Defic Syndr 46:564–573. doi: 10.1097/QAI.0b013e318159d807 [PubMed: 18193498]

Stubbe-Drger B, Deppe M, Mohammadi S, Keller SS, Kugel H, Gregor N, Evers S, Young P, Ringelstein EB, Arendt G, Knecht S, Husstedt IW; German Competence Network HIV/AIDS (2012) Early microstructural white matter changes in patients with HIV: a diffusion tensor imaging study. BMC Neurol 12:23. doi: 10.1186/1471-2377-12-23 [PubMed: 22548835]

Thomason ME, Thompson PM (2011) Diffusion imaging, white matter and psychopathology. Ann Rev Clin Psychol 7:63–85. doi: 10.1146/annurev-clinpsy-032210-104507 [PubMed: 21219189]

Thurnher MM, Castillo M, Stadler A, Rieger A, Schmid B, Sundgren PC (2005) Diffusion-tensor MR imaging of the brain in human immunodeficiency virus-positive patients. AJNR Am J Neuroradiol 26:2275–2281. [PubMed: 16219833]

Uban KA, Herting MM, Williams PL, Ajmera T, Gautam P, Huo Y, Malee KM, Yogev R, Csernansky JG, Wang L, Nichols SL, Sowell ER; Pediatric HIVAIDS Cohort and the Pediatric Imaging, Neurocognition, and Genetics Studies (2015) White matter microstructure among youth with perinatally acquired HIV is associated with disease severity. AIDS 29:1035–1044. doi: 10.1097/QAD.0000000000000648 [PubMed: 26125138]

Wang Y, Wang Q, Haldar JP, Yeh FC, Xie M, Sun P, Tu TW, Trinkaus K, Klein RS, Cross AH, Song SK (2011) Quantification of increased cellularity during inflammatory demyelination. Brain 134:3587–3598. doi: 10.1093/brain/awr307

Whitehead N, Potterton J, Coovadia A (2014) The neurodevelopment of HIV-infected infants on HAART compared to HIV-exposed but uninfected infants. AIDS Care 26:497–504. doi: 10.1080/09540121.2013.841828 [PubMed: 24125015]

Winston A, Puls R, Kerr SJ, Duncombe C, Li P, Gill JM, Ramautarsing R, Taylor-Robinson SD, Emery S, Cooper DA, ALTAIR Study Group (2015) Differences in the direction of change of cerebral function parameters are evident over three years in HIV-infected individuals electively commencing initial cART. PLoS One 10:e0118608. doi: 10.1371/journal.pone.0118608 [PubMed: 25723494]

Wood SP, Moore DJ, Weber E, Grant I (2009) Cognitive neuropsychology of HIV-associated neurocognitive disorders. Neuropsychol Rev 19:152–168. doi: 10.1007/s11065-009-9102-5 [PubMed: 19462243]

Wozniak JR, Lim KO (2006) Advances in white matter imaging: a review of in vivo magnetic resonance methodologies and their applicability to the study of development and aging. Neurosci Biobehav Rev 30:762–774. doi: 10.1016/j.neubiorev.2006.06.003 [PubMed: 16890990]

Wright PW, Heaps JM, Shimony JS, Thomas JB, Ances BM (2012) The effects of HIV and combination antiretroviral therapy on white matter integrity. AIDS 26:1501–1508. doi: 10.1097/QAD.0b013e3283550bec [PubMed: 22546990]

Wu Y, Storey P, Cohen BA, Epstein LG, Edelman RR, Ragin AB (2006) Diffusion alterations in corpus callosum of patients with HIV. AJNR Am J Neuroradiol 27:656–660. https://www.fil.ion.ucl.ac.uk/spm/software/spm12/. [PubMed: 16552012]

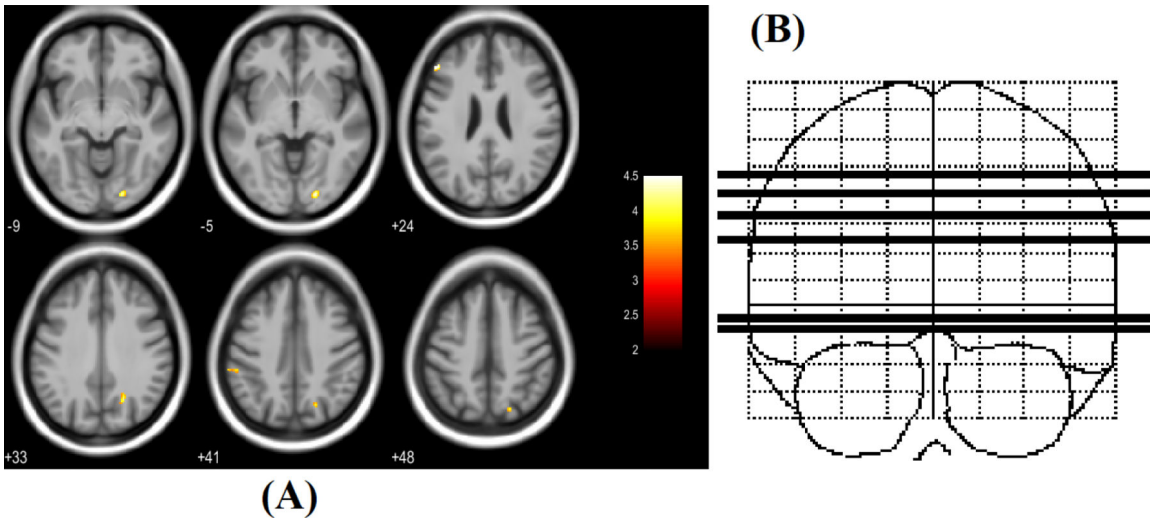

Figure 1:

(A) Regions of significantly increased FA in PHIV-infected youths compared to healthy controls (red-yellow, scaled by t statistic). Significance thresholds were set for $P < 0.001$ (uncorrected for multiple comparisons), with an extent threshold of 30 voxels for the analysis. Voxels evidencing significant differences in FA are displayed on axial sections of a canonical brain image. The right side of the images represent the right side of the brain. Numbers indicate Z coordinates in mm relative to the SPM template. **(B)** Sketch indicating location of 6 axial slices in coronal plane.

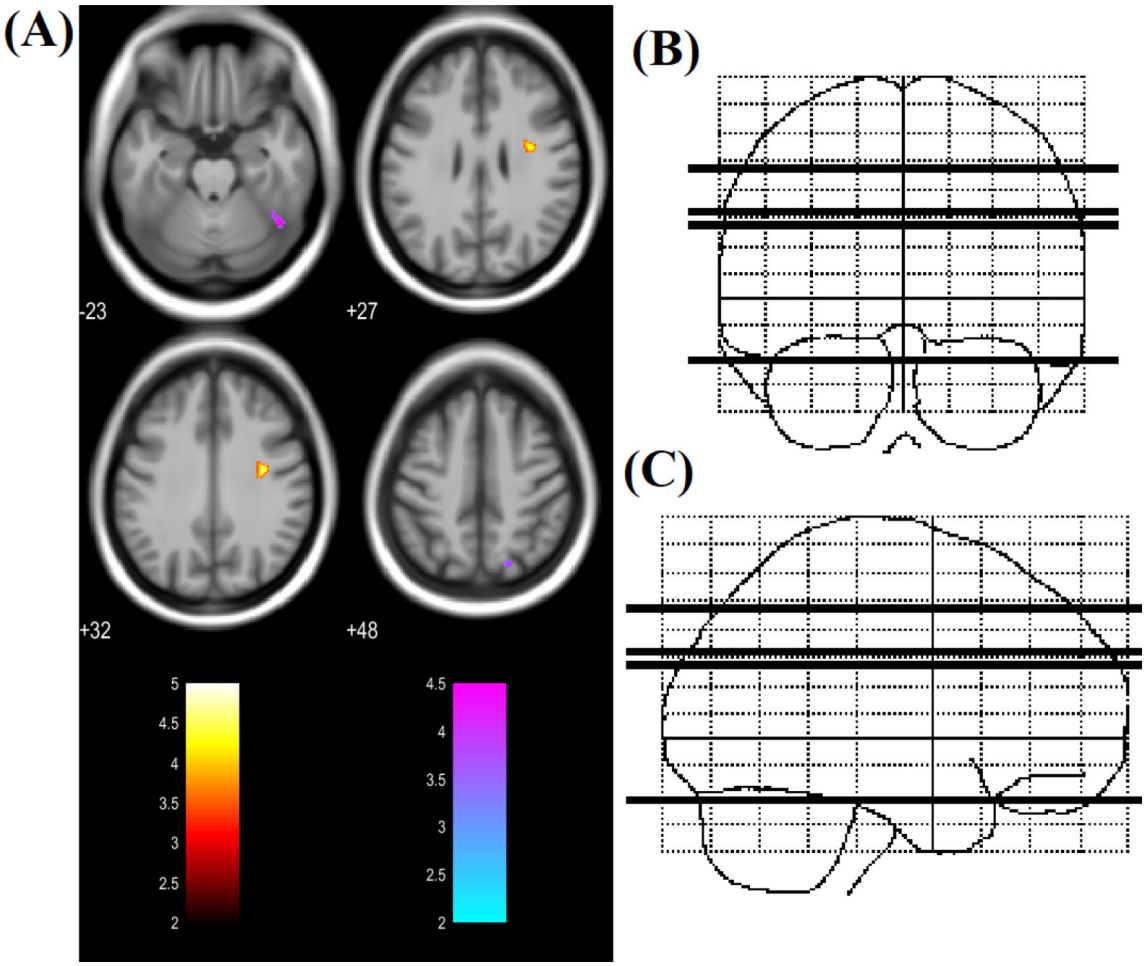

Figure 2:

(A) Regions of significantly increased MD (red to yellow) and decreased MD (blue to green) in PHIV-infected youths compared to healthy controls (t-statistic scale). Significance thresholds were set for $P < 0.001$ (uncorrected for multiple comparisons), with an extent threshold of 30 voxels for both analyses. Voxels evidencing significant differences in MD are displayed on axial sections on a canonical brain image with the color scale indicating the magnitude of Z values. The right side of the images represent the right side of the brain. Numbers indicate Z coordinates in mm relative to the SPM template. **(B) & (C)** Sketch indicating location of 4 axial slices in coronal and sagittal plane respectively.

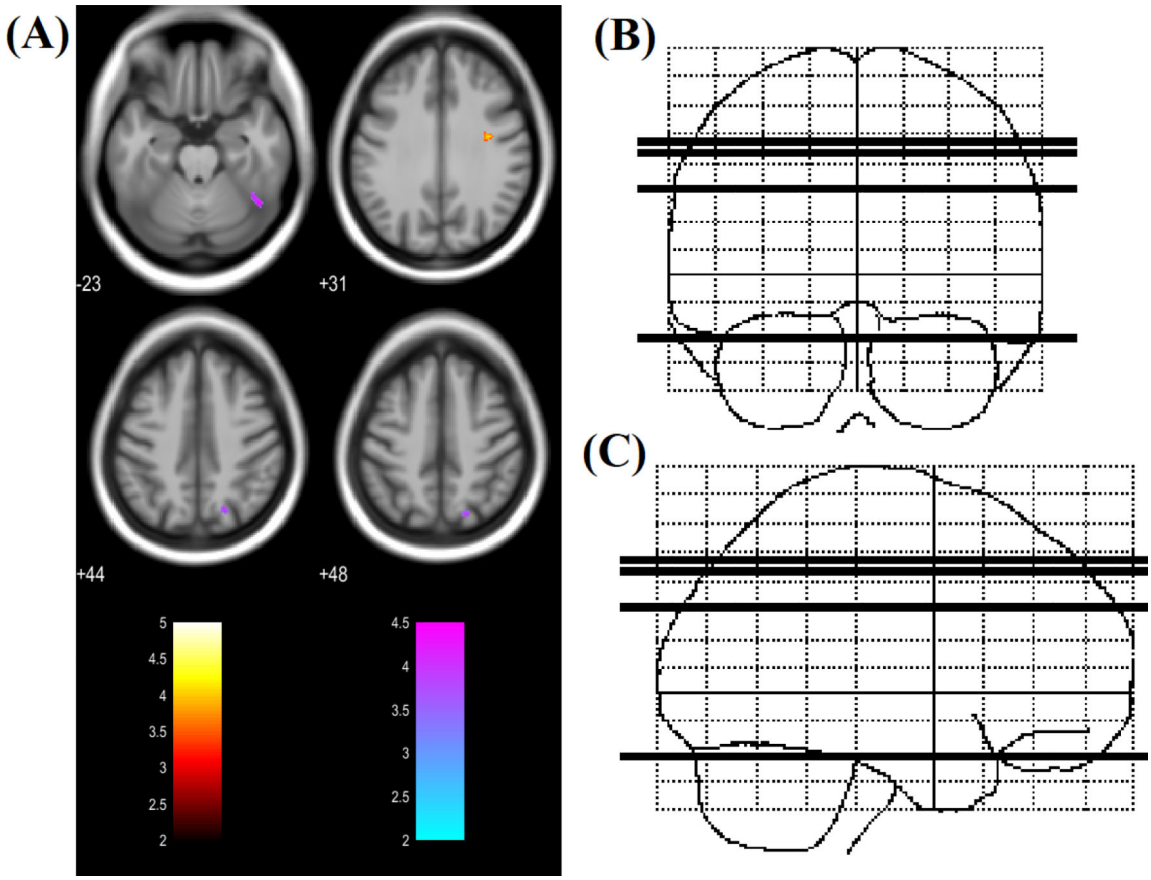

Figure 3:

(A) Regions of significantly increased RD (red to yellow) and decreased RD (blue to green) in PHIV-infected youths compared to healthy controls (t-statistic scale). Significance thresholds were set for $P < 0.001$ (uncorrected for multiple comparisons), with an extent threshold of 30 voxels for both analyses. Voxels evidencing significant differences in RD are displayed on axial sections of a canonical brain image with the color scale indicating the magnitude of Z values. The right side of the images represent the right side of the brain. Numbers indicate Z coordinates in mm relative to the SPM template. **(B) & (C)** Sketch indicating location of 4 axial slices in coronal and sagittal plane respectively.

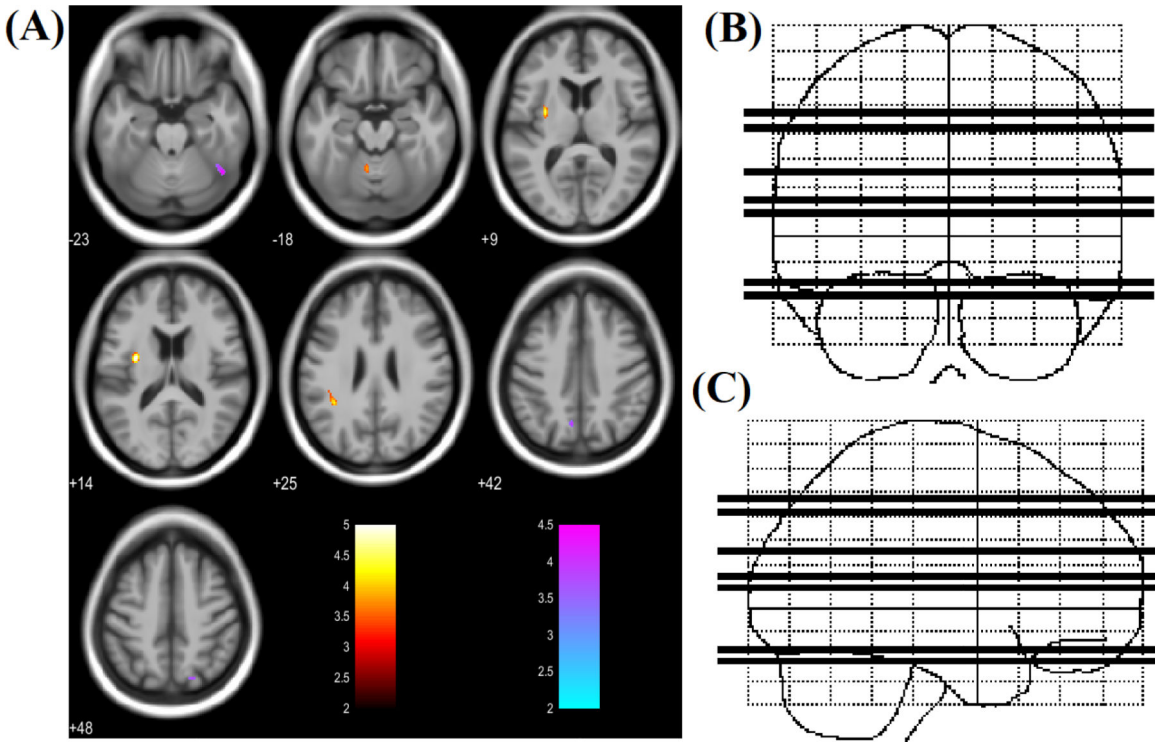

Figure 4:

(A) Regions of significantly increased AD (red to yellow) and decreased AD (blue to green) in PHIV-infected youths compared to healthy controls (t-statistic scale). Significance thresholds were set for $P < 0.001$ (uncorrected for multiple comparisons), with an extent threshold of 30 voxels for both analyses. Voxels evidencing significant differences in AD are displayed on axial sections of a canonical brain image with the color scale indicating the magnitude of Z values. The right side of the images represent the right side of the brain. Numbers indicate Z coordinates in mm relative to the SPM template. **(B) & (C)** Sketch indicating location of 7 axial slices in coronal and sagittal plane respectively.

Table 1:

Demographic and clinical characteristics of PHIV-infected youths and healthy controls. P-value shown for group differences assessed with independent samples t-test (age) or chi-square (sex distribution).

Characteristics	PHIV-infected (n=14)	Healthy (n=17)	P-value
Age (years)	17.92 ± 2.48	17.95 ± 2.95	0.97
Sex (Male : Female)	5 : 9	7 : 10	0.77
CD4 T-cell count	630.18 ± 307.45	-	-
Age at ART initiation (months)	59.71 ± 57.31	-	-
Age at HIV diagnosis (months)	51.64 ± 53.41	-	-
Duration ART (months)	155.35 ± 64.68	-	-
Log viral load < 1.68	10	-	-

Table 2:

Regional FA, MD, RD and AD value changes in PHIV youths compared to healthy control.

Regions	PHIV Youth	Healthy Control	P-value
FA			
Left middle frontal gyrus	0.22 ± 0.05	0.16 ± 0.02	**≤0.001**
Right precuneus	0.36 ± 0.06	0.25 ± 0.07	**≤0.001**
Right lingual gyrus	0.33 ± 0.08	0.21 ± 0.06	**≤0.001**
Left supramarginal gyrus	0.23 ± 0.05	0.18 ± 0.03	0.001
MD ($\times 10^{-3}$ mm^2.s^{-1})			
Right precentral gyrus	0.73 ± 0.05	0.68 ± 0.04	0.002
Right superior parietal lobule	0.86 ± 0.11	1.16 ± 0.28	**≤0.001**
Right inferior temporal gyrus/fusiform gyrus	1.00 ± 0.12	1.29 ± 0.17	**≤0.001**
RD ($\times 10^{-3}$ mm^2.s^{-1})			
Right precentral gyrus	0.56 ± 0.05	0.51 ± 0.04	0.018
Right superior parietal lobule	0.74 ± 0.14	1.07 ± 0.32	**≤0.001**
Right inferior temporal gyrus/fusiform gyrus	0.90 ± 0.13	1.20 ± 0.16	**≤0.001**
AD ($\times 10^{-3}$ mm^2.s^{-1})			
Left Putamen	1.12 ± 0.06	1.04 ± 0.05	**≤0.001**
Left parietal operculum	1.16 ± 0.08	1.06 ± 0.06	0.012
Cerebellar Vermal Lobules	1.03 ± 0.10	0.96 ± 0.08	0.010
Right inferior temporal gyrus/fusiform gyrus	1.22 ± 0.14	1.54 ± 0.19	**≤0.001**
Right posterior cingulate gyrus	2.10 ± 0.81	2.72 ± 0.81	0.027
Right superior parietal lobule	1.13 ± 0.08	1.38 ± 0.27	**≤0.001**
Left precuneus	1.06 ± 0.10	1.15 ± 0.12	0.025